Available online at www.sciencedirect.com

ScienceDirect

Procedia Engineering 103 (2015) 444 – 449

Procedia Engineering

www.elsevier.com/locate/procedia

The 13th Hypervelocity Impact Symposium

Ejecta Cone Angle and Ejecta Size Following a Non-Perforating Hypervelocity Impact

Masahiro Nishida[a]*, Yasuyuki Hiraiwa[a], Koichi Hayashi[b], Sunao Hasegawa[c]

[a]*Nagoya Institute of Technology, Gokiso-cho, Showa-ku, Nagoya 466-8555, Japan*
[b]*Toba National College of Maritime Technology, 1-1 Ikegami-cho, Toba, Mie, 517-8501 Japan*
[c]*Institute of Space and Astronautical Science, Japan Aerospace Exploration Agency, 3-1-1, Yoshinodai,Chuo-ku, Sagamihara, Kanagawa, 252- 5210 Japan*

Abstract

The effects of projectile diameter and impact velocity on ejecta cone angle and ejecta size distribution were investigated by striking aluminum alloy 6061-T6 targets with aluminum alloy 2017-T4 spheres at velocities ranging from 2 to 6 km/s. The two-stage light-gas gun at the Institute of Space and Astronautical Science (ISAS)/ Japan Aerospace Exploration Agency (JAXA), and Nagoya Institute of Technology was used for the experiments. To examine the scattering angles of ejecta, a witness plate (150 mm × 150 mm, 2 mm in thickness) made of copper C1100P-1/4H, with a 30-mm hole in the center, was placed 50 mm in front of the target.

Peer-review under responsibility of the Curators of the University of Missouri On behalf of the Missouri University of Science and Technology

Keywords: Ejecta length; Ejecta ring; Scalling law; No perforation; Cratering

1. Introduction

Space debris often strikes space stations and spacecraft at hypervelocities. The International Space Station (ISS) employs shields, such as the Whipple shield, which consists of thin plates to protect itself from space debris. When space debris perforates thin plates, debris clouds are formed. In comparison, space debris with low kinetic energy—those with a small size or low velocity—do not perforate the bumpers and outer surfaces of spacecraft and space stations; instead, they form craters on these surfaces. In such a case, all projectile and target materials can only be ejected in the reverse direction at almost the same time as the growth of the crater. Fragments ejected from the target surface and fragmented projectile are scattered widely. These ejecta and fragments have the potential to become space debris (known as secondary debris).

Several studies have been carried out on the formation and structure of such ejecta and fragments. Schonberg studied spatial distributions of ricochet debris cloud spray and trajectory angles when projectiles struck thin plats at hypervelocities [1, 2]. Murr *et al.* studied projectile fragments and ejected materials in detail [3]. Takayama's group of Tohoku University in Japan studied the ejecta composition [4]. With respect to spacecraft and rocket bodies in low Earth orbit (LEO), NASA's breakup model was proposed [5, 6]. On the other hand, the international standard for test procedures to evaluate spacecraft material ejecta was published in 2012 [7]. Some studies have been conducted on related phenomena [8, 9]. However, the size distributions of the ejecta and fragments have not yet been fully elucidated.

In this study, we investigated the effects of projectile diameter and impact velocity on ejecta cone angle and ejecta size distribution when spherical projectiles made of aluminum alloy 2017-T4 impact thick targets made of aluminum alloy 6061-

* Masahiro Nishida. Tel.: +81-52-735-5349; fax: +81-52-735-5503.
E-mail address: nishida.masahiro@nitech.ac.jp

Peer-review under responsibility of the Curators of the University of Missouri On behalf of the Missouri University of Science and Technology
doi:10.1016/j.proeng.2015.04.058

T6 at hypervelocities. We examined scaling law for ejecta cone angle and ejecta size distribution. In the field of solar system studies, many studies have been conducted on scaling model for the ejecta mass and velocity distribution of rocky materials. (For example, [10, 11]) We examined the scaling law of ductile materials by reference to earlier studies about rocky materials.

2. Experimental Methods

The two-stage light-gas guns at the Institute of Space and Astronautical Science (ISAS)/Japan Aerospace Exploration Agency (JAXA) [12] and Nagoya Institute of Technology, was used at velocities ranging from 2 to 6 km/s. Three types of projectiles with diameters of 1.6 mm, 3.2 mm and 7 mm made of aluminum alloy 2017-T4 were used. Thick targets with a thickness of 30 mm made of aluminum alloy 6061-T6 were employed. After impact experiments, the size of ejecta collected from the test chamber was measured. We did not use any special devices and media to collect ejecta. Ejecta fallen on the floor of test chamber were collected to measure the size of the ejecta. We examined the effects of the projectile diameter and impact velocity on distribution of ejecta size. A witness plate (150 mm×150 mm, 2 mm in thickness) made of copper, C1100P-1/4H, with a hole of 30 mm in diameter was placed 50 mm in front of each target, as shown in Fig. 1. We examined the effects of the projectile diameter and impact velocity on ejecta cone angle using crater size due to ejecta impact on witness plates.

The size (length *a*, width *b*, thickness *c*) of ejecta was defined as shown in Fig. 2. The length, *a* was calculated from a photograph of each ejecta using image analysis software (ImageJ). The length, *a*, and width, *b*, were selected by image analysis software, ImageJ, so as to be normal to each other.

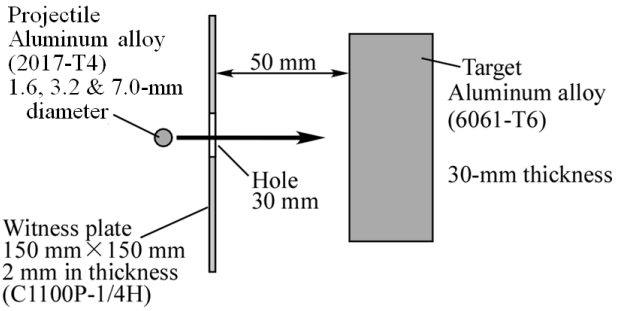

Fig. 1. Experimental setup for projectile impact.

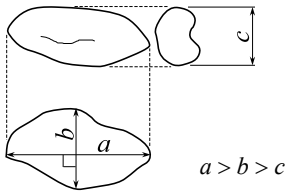

Fig. 2. Experimental setup for projectile impact.

3. Results and Discussion

Figure 3 shows a photograph of ejecta collected from test chamber when a projectile of 7.0 mm in diameter struck a target at an impact velocity of 3.57 km/s. We could collect ejecta from the target and fragments from the projectile. After a photograph of each ejecta was taken, ejecta size was calculated using the image analysis software, ImageJ. Cumulative number of ejecta length was examined.

Figure 4(a) shows the cumulative number distribution of ejecta length, *a*, at an impact velocity of approximately 2 km/s. In this figure, the cumulative number of ejecta length means the number of ejecta with a length greater than the length of ejecta on the horizontal axis. For example, when the projectile diameter was 7 mm, black dots, the cumulative number of ejecta having the length over 0.5 mm on the horizontal axis was 210. In this study, collection rates of ejecta were 50-70%. Here, collection rates mean the weight ratios of total ejecta mass collected from test chamber to the sum of initial projectile

mass and decreased mass of target. As one can easily predict, the maximum length and the cumulative number increased with increasing projectile diameter. Then, the scaling law of ejecta length distribution was considered. In Fig. 4(b), when ejecta length on the horizontal axis was divided by projectile diameter, results of three projectile diameters were roughly on a curve. The projectile diameter seems to be important for ejecta length. When the ejecta length of all experimental results was normalized by projectile diameter on the horizontal axis as shown in Fig. 4(c), the cumulative number distributions were divided into three groups according to the impact velocity. The cumulative number of ejecta length on the vertical axis increased with increasing impact velocity.

Because the cumulative number of ejecta length increased with impact velocity, we considered the effects of the impact velocity of the projectiles. The vertical axis was divided by exponentiation of impact velocity, for example impact velocity to the power 1.5 or the square of impact velocity. When the vertical axis was divided by the impact velocity to the power 1.5, all the results at three impact velocities were roughly on a curve. Interestingly, the cumulative number of ejecta length seems to be proportional to the impact velocity to the power 1.5 as shown in Fig. 4(d).

Fig. 3. Photograph of ejecta collected from test chamber (Projectile of 7.0 mm in diameter, impact velocity 3.57 km/s).

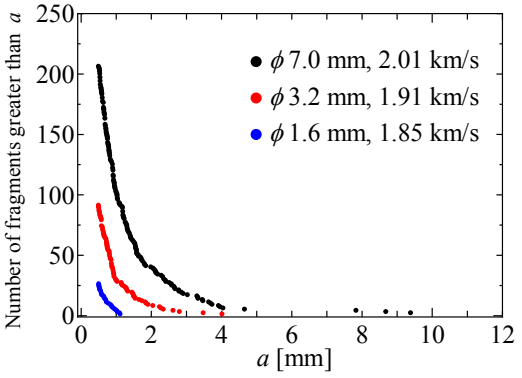

(a) Effect of projectile density

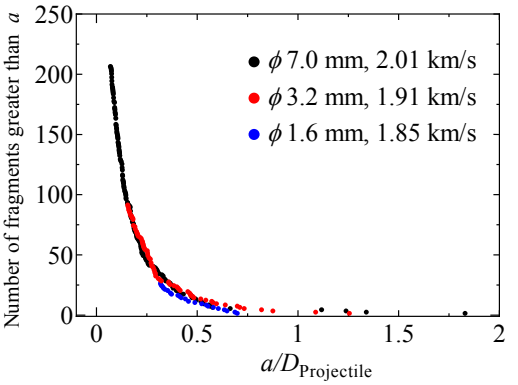

(b) Normalization of horizontal axis

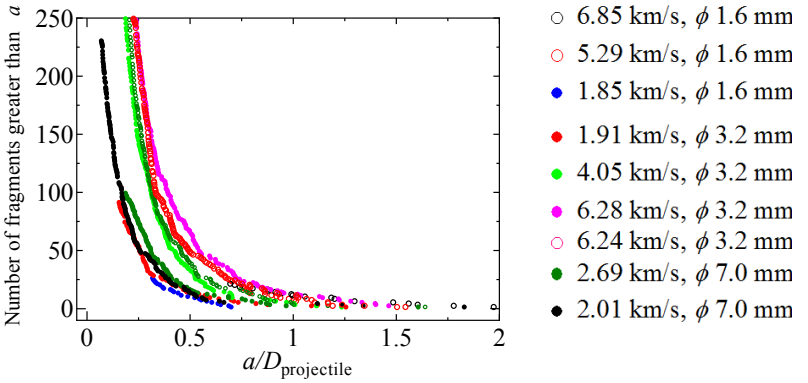

(c) Effect of impact velocity

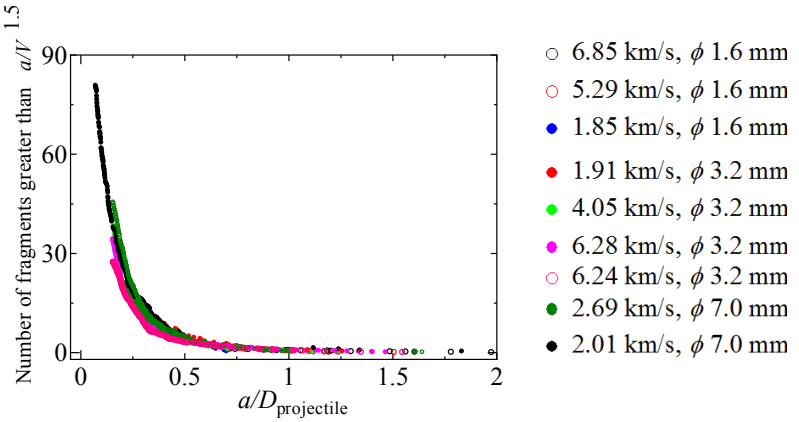

(d) Normalization of vertical axis

Fig. 4. Cumulative number distribution of ejecta length *a*.

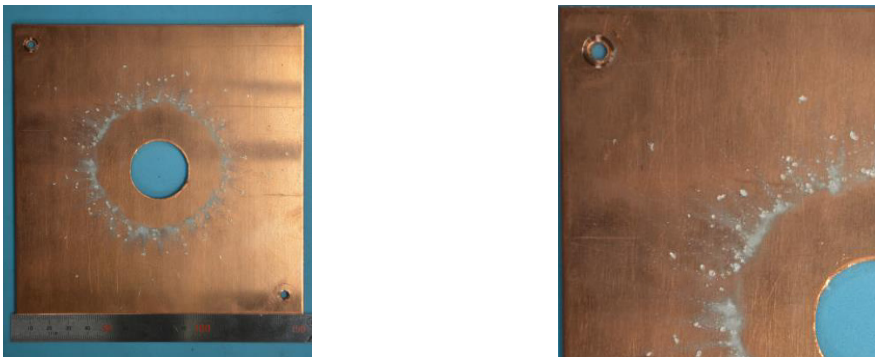

(a) Whole plate (b) Enlarged image of one-fourth part

Fig. 5 Observation of craters due to ejecta impact on witness plates (Projectile of 3.2 mm in diameter, impact velocity 4.88 km/s).

Images of the witness plates after the experiments are shown in Fig. 5. We could observe a ring area consisting of many indentations (white indentations) due to impact of ejecta. In addition to these, outside of the ring area, we could observe many radial indentations. Based on earlier stud studies and our results, the authors group developed a hypothesis as shown in Fig. 6 about the ejecta composition consisting of four parts; starting from the central axis of the ejecta cone and moving outward: (1) fragmented or melted projectile fragments, most of which have pass through the hole again in Fig. 5, (2) a ring area of many small fragments, (3) larger fragments that broke from the crater lip, and (4) radial scattered fragments outside the ring [13].

The inner diameter, D_{ej}, of ring areas defined in Fig. 7 was measured. The scatter angle was examined. The scatter angle of the ejecta fragments, ϕ, defined as the angle shown in Fig. 8

$$\phi = \tan^{-1}\left(\frac{D_{ej} - d_c}{2} \times \frac{1}{50}\right) \tag{1}$$

Here, the ejecta ring diameter D_{ej} (mm) and the final crater diameter d_c (mm). 50 mm is the distance between witness plate and target. Note that d_c is not the diameter of the transient crater.

The scatter angle decreased gradually with increasing impact velocity, and the projectile diameter slightly increased the scatter angle. However, there seems to be no significant difference in diameter. The scatter angle approached approximately 25° as the impact velocity increased. Mandeville and Bariteau [14] showed that the elevation angle of the ejecta cone is approximately 60° and small and fast particles are ejected at a constant elevation angle. Because 60° in their definition is

equivalent to 30° in Fig. 8, Mandeville and Bariteau did not mention the effects of impact velocity of projectile; however, in Fig. 9, the angle of the ejecta cone clearly depended on the impact velocity under our experimental conditions.

We expected that the hardness, tensile strength and/or elongation at break would affect the scatter angle of the ejecta fragments. However, it is not clear how such factors affect the scatter angle, and more detailed investigations into ejecta formation including scatter angle are required. By applying an index of exponential function to the experimental results, $D_{ej} \sim V^{-0.50}$ could be obtained.

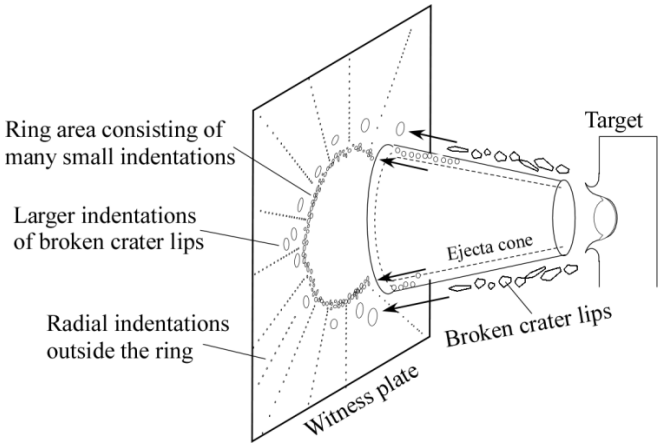

Fig. 6 Schematic diagram of ejecta composition and indentation on witness plate; a ring area of crates due to impact of many small fragments, larger indentations due to fragments that broke from the crater lip, and radial indentations outside the ring.

Fig. 7 Inner diameter of ejecta ring, D_{ej}

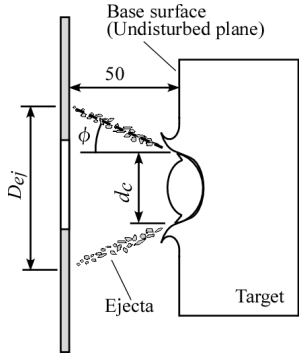

Fig. 8 Definition of ejecta scatter angle using ejecta ring diameter and final crater diameter.

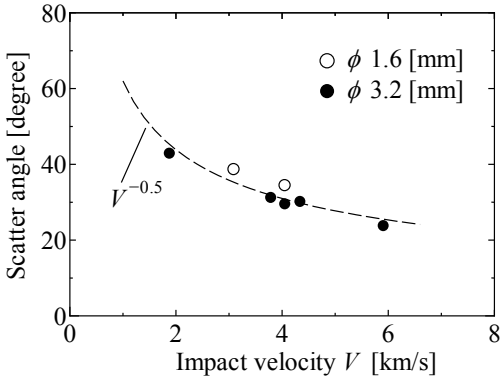

Fig. 9 Effects of impact velocity on scatter angle

4. Conclusion

The effects of projectile diameter and impact velocity on ejecta cone angle and ejecta size distribution were examined when spherical projectiles made of aluminum alloy 2017-T4 impact thick targets made of aluminum alloy 6061-T6 at hypervelocities. When the ejecta length on the horizontal axis was divided by the projectile diameter, the cumulative number of normalized ejecta length was proportional to the impact velocity to the power 1.5. The scatter angle decreased gradually with increasing impact velocity. The scatter angle converges to approximately 25°.

Acknowledgements

This work was supported by the Space Plasma Laboratory, ISAS, JAXA as a collaborative program with the hypervelocity impact experiment. This work was supported in part by a Grant-in-Aid for Scientific Research (C), KAKENHI (26420012), from the Japan Society for the Promotion of Science (JSPS).

References

[1] Schonberg, W.P. , Taylor, R.A, 1989. Oblique Hypervelocity Impact Response of Dual-sheet Structures, NASA TM-100358.
[2] Schonberg, W. P., 2001. Characterizing Secondary Debris Impact Ejecta, International Journal of Impact Engineering, 26, pp. 713-724.
[3] Hernandez, V.S., Murr, L.E., Anchondo, I.A., 2006. Experimental Observations and Computer Simulations for Metallic Projectile Fragmentation and Impact Crater Development in Thick Metal Targets, International Journal of Impact Engineering, 32, pp. 1981-1999.
[4] Numata, D., Kikuchi, T., Sun, M., Kaiho, K., Takayama, K., 2006. Experimental Study of Impact Ejecta Composition Using a Ballistic Range, Proc of JSSW, pp. 221-222.
[5] Johnson, N.L., Krisko, P.H., Liou, J.-C., Anz-Meador, P.D., 2001. NASA's New Breakup Model of EVOLVE 4.0, Advances in Space Research, 28, pp. 1377-1384.
[6] Liou, J.-C., Johnson, N. L., Krisko, P. H., Anz-Meador, P. D., 2002. The New NASA Orbital Debris Breakup Model. In: Green, S.F. et al. editors, Dust in the Solar System and Other Planetary Systems, Pergamon, London, UK, pp. 363-367.
[7] ISO 11227, 2012. Space systems - Test Procedure to Evaluate Spacecraft Material Ejecta upon Hypervelocity Impact.
[8] Sugahara, K., Aso, K., Akahoshi, Y., Koura, T. and Narumi, Y. (2009). Intact Measurement of Fragments in Ejecta Due to Hypervelocity Impact. Proc. 60th Int. Astronautical Cong. IAC-09-A6.3.06.
[9] Siguier, J.M. and Mandeville, J.C. (2007). Test Procedures to Evaluate Space Materials Ejecta upon Hypervelocity Impact. Proc. IMechE. G, 221, pp. 969-974,
[10] Holsapple, K., Giblin, I., Housen, K., Nakamura, A., Ryan, E., 2002. Asteroid Impacts: Laboratory Experiments and Scaling Laws, Asteroids III, W. F. Bottke Jr., A. Cellino, P. Paolicchi, and R. P. Binzel (eds), University of Arizona Press, Tucson, p.443-462.
[11] Housen, K.R., Holsapple, K.A., 2011. Ejecta from Impact Craters, Icarus, 211, pp. 856-875.
[12] Kawai, N., Tsurui, K., Hasegawa, S., Sato, E., 2010. Single Microparticle Launching Method Using Two-Stage Light-Gas Gun for Simulating Hypervelocity Impacts of Micrometeoroids and Space Debris, Review of Scientific Instruments, 81, 115105.
[13] Nishida, M., Kuzuya, K., Hayashi, K., Hasegawa, S., 2013. Effects of Alloy Type and Heat Treatment on Ejecta and Crater Sizes in Aluminum Alloys Subjected to Hypervelocity Impacts, International Journal of Impact Engineering, 54, pp. 161-176.
[14] Mandeville, J. C., Bariteau, M., 2004. Contribution of Secondary Ejecta to the Debris Population, Advances in Space Research, 34, pp. 944-950.